

# Coupling a glacier melt model to the Variable Infiltration Capacity (VIC) model for hydrological modeling in north-western China

Qiudong Zhao · Baisheng Ye · Yongjian Ding ·  
Shiqiang Zhang · Shuhua Yi · Jian Wang ·  
Donghui Shangguan · Chuancheng Zhao · Haidong Han

Received: 26 May 2011 / Accepted: 10 May 2012 / Published online: 24 May 2012  
© Springer-Verlag 2012

**Abstract** For the sustainable utilization of rivers in the mid and downstream regions, it is essential that land surface hydrological processes are quantified in high cold mountains regions, as it is in these regions where most of the larger rivers in China acquire their headstreams. Glaciers are one of the most important water resources of north-west China. However, they are seldom explicitly considered within hydrological models, and climate-change effects on glaciers, permafrost and snow cover will have increasingly important consequences for runoff. In this study, an energy-balance ice-melt model was integrated within the Variable Infiltration Capacity (VIC) macroscale hydrological model. The extended VIC model was applied to simulate the hydrological processes in the Aksu River basin, a large mountainous and glaciated catchment in north-west China. The runoff components and their response to climate change were analyzed based on the simulated and observed data. The model showed an acceptable performance, and achieved an efficiency coefficient  $R^2 \approx 0.8$  for the complete simulation period. The results indicate that a large proportion of the catchment runoff is derived from ice meltwater and snowmelt water. In addition, over the last 38 years, rising temperature

caused an extension in the snow/ice melting period and a reduction in the seasonality signal of runoff. Due to the increased precipitation runoff, the Aksu catchment annual runoff had a positive trend, increasing by about  $40.00 \times 10^6 \text{ m}^3$  per year, or 25.7 %.

**Keywords** Energy-balance glacier melt model · Variable Infiltration Capacity (VIC) macroscale hydrologic model · Aksu River basin · Hydrological modeling

## Introduction

In north-western China, mountain glaciers and seasonal snowpack play an important role in the hydrological cycle. These watersheds in mountainous areas form the headwaters of rivers that provide water to some of the most populated areas, especially in arid and semi-arid inland river basins (Kang et al. 1999; Chen et al. 2006). In the cold regions of the north-western China, global warming has resulted in the universal receding of glacial and permafrost regions. In addition, changes in ecosystems and the microclimate environment cause changes in runoff generation processes and total runoff (Yang et al. 2000; Barnett et al. 2005). In the long run, continuing loss of glacial mass will raise the risk of low-flow periods in arid and semiarid regions, while in the short term, the intensification of glacial melt will lead to an increasing risk of local flooding during the summer season, when peak flows increase dramatically (Higuchi 1976, 1977, 1978, 1980; Braun et al. 2000; Hock et al. 2005).

Globally, glacial melt represents a very significant source of streamflow in high-mountain regions (Hock et al. 2005). The glacial storage of water as snow and ice results in glacier hydrology differing significantly from the

Q. Zhao (✉) · Y. Ding · J. Wang · C. Zhao · H. Han  
Division of Hydrology and Water-Land Resource in Cold and Arid Regions, Cold and Arid Regions Environmental and Engineering Research Institute, Chinese Academy of Sciences, Lanzhou, China  
e-mail: dsslab@163.com

Q. Zhao · B. Ye · Y. Ding · S. Zhang · S. Yi · D. Shangguan  
The State Key Laboratory of Cryospheric Sciences,  
Cold and Arid Regions Environmental and Engineering  
Research Institute, Chinese Academy of Sciences,  
Lanzhou, China

conventional hydrology with regard to the volume, timing, and variability of streamflows. In the mid latitudes, glacial runoff can amplify the seasonality of runoff, while in low-latitude high-mountain areas, the effect of glacial melt can cause the seasonality of runoff to be less pronounced (Kaser et al. 2003). The success of modeling the glacier-derived runoff strongly depends on the formulation of the melt processes. During the last few decades, a large variety of melt models have been developed ranging from simple temperature index to sophisticated energy-balance models (Hock et al. 2005). Temperature-index models have been the most common approach for melt modeling due to the extensive availability of air temperature data and simplicity of computation. Temperature-index methods have a wide range of applications, including prediction of melt for operational flood forecasting and hydrological modeling (WMO 1986). Temperature-index methods for melt modeling have been adopted by most operational runoff models, e.g., the HBV model (Bergström 1976), the SRM model (Martinec and Rango 1986), the UBC model (Quick and Pipes 1977), the HYMET model (Tangborn 1984) and the SHE model (Bøggild et al. 1999). However, the use of temperature-index methods to estimate the ablation neglects sublimation and other potentially important variables such as radiation, wind speed, relative humidity and cloud cover. In addition, the approach assumes snow and ice melt at 0 °C (Rupper and Roe 2008), however, the onset of melt is determined by the surface-energy balance, which is only indirectly affected by air temperature (Hock 2005). This type of approach requires the use of a melt factor that relates the measure of summer temperature to the ablation rate. The melt factor is an empirically determined parameter. Yet, studies of different glaciers suggest that melt factors vary from place to place by a factor of up to five (Kayastha et al. 2003; Zhang et al. 2006). A more physically based approach to modeling ablation is the energy-balance method for calculating the melt of ice/snow. The advantage of this method is that it considers all relevant atmospheric variables and calculates the melting and sublimation of ice/snow. The method has been applied successfully at a variety of scales ranging from single glaciers and basins to whole complexes of glaciers across large regions (Mölg and Hardy 2004). Some studies show that glaciers are sensitive to changes in temperature, precipitation and moisture-related variables, such as cloudiness and relative humidity (Hastenrath 1994; Mölg and Hardy 2004).

Frozen soil (permafrost and seasonally frozen soil) processes are critically important in the land-surface hydrology in cold regions, since the freeze–thaw cycle significantly alters the soil hydraulic and thermal characteristics, resulting in direct effects on the water and energy cycles on the land surface (Wang et al. 2010; Ye et al.

2009). So far, many studies have made efforts to improve the frozen soil parameterization in land-surface modeling (Betts et al. 1996; Cherkauer and Lettenmaier 1999; Smirnova et al. 2000; Li and Koike 2003; Yi et al. 2006, 2007; Zhang et al. 2007; Nicolsky et al. 2007; Chen et al. 2008; Luo et al. 2009). One of the first models coupling heat and water fluxes for a layered soil profile was developed by Harlan (1973). The SHAW and VIC models (Flerchinger and Saxton 1989; Cherkauer and Lettenmaier 1999, 2003) extended Harlan's concept to include detailed soil–vegetation–atmosphere transfer (SVAT) schemes including a process description of soil freezing and thawing.

Runoff from mountainous watersheds is one of the main water sources for inland river basins of the arid and semi-arid regions of the north-west China. The prediction of flow discharge in mountainous watersheds is essential to sustainable development in the more arid mid- and downstream regions. In the past decade, distributed, physically based hydrological models (DHSVM, MIKE SHE, WAT-FLOOD, IISDHM, VIC, etc. (for review, see Storck 2000; Liang et al. 1994; Beven 2001) have become established tools for studying the hydrological cycle, considering its present state and possible future changes in climate and land use from spatial scales of individual basin to a global scale (Barnett et al. 2005; Singh and Bengtsson 2005; Christensen and Lettenmaier 2007; Viviroli et al. 2007). The physically based distributed models incorporate streamflow, precipitation, evaporation, averaged stochastic groundwater flow and spatial properties of the catchment such as elevation data, topographic indices, glacier grid, land use, and soil types. However, few distributed hydrological models have been designed specially for cold mountain regions where the frozen soil, snow and glacier hydrological processes are critical to streamflow. Abundant studies aim to simulate snowmelt-induced runoff (Martinec and Rango 1986; Li and Williams 2008; Zhao et al. 2009), but there is a lack of focus on the modeling of glacial discharge (Hock 1998; Hock and Holmgren 2005). In addition, most existing soil water transfer models do not include frost effects (Bayard and Stähli 2005).

The Variable Infiltration Capacity (VIC) macroscale hydrologic model is a surface-water and energy-balance model designed for large-scale applications. It is applied to grid cells, typically with spatial dimensions from 1/8° to 2° latitude by longitude, connected so as to represent large continental river basins (Liang et al. 1994, 1996; Nijssen et al. 2001; Bowling et al. 2004; Costa-Cabral et al. 2008). The model is distinguished from other Soil vegetation atmosphere transfer (SVAT) schemes by its focus on runoff processes. Over the last several years, a number of changes have been made to improve the VIC model's representation in cold regions, in conjunction with the Global Energy and

Water-balance Experiment (GEWEX) Continental-scale International Project (GCIP) activities in the upper Mississippi River basin (Cherkauer and Lettenmaier 1999). An algorithm to represent the effects of frozen soil, the addition of an algorithm to simulate the interception of snow by forest canopies, and general improvements to the snow accumulation and ablation algorithm have been incorporated into the VIC model (Cherkauer and Lettenmaier 2003). Unfortunately, there is no incorporation of a glacier mass-balance model in the VIC model to model the mountain hydrological processes in north-west China, especially in highly glaciated mountain areas.

The first purpose of this study was to couple a glacier energy and mass-balance algorithm to the VIC model for improving the model performance in cold mountain catchments. Subsequently, this study applied the extended VIC model to simulate the intra- and inter-annual variability of runoff within the calibration period (1980–1989) and validation period (1970–2007) in a large mountain catchment area in north-west China. Runoff was simulated at daily time steps to explore the varying characteristics of the runoff components (including the glacial runoff, snowmelt runoff and rainfall runoff) during the 38 years.

**Model description**

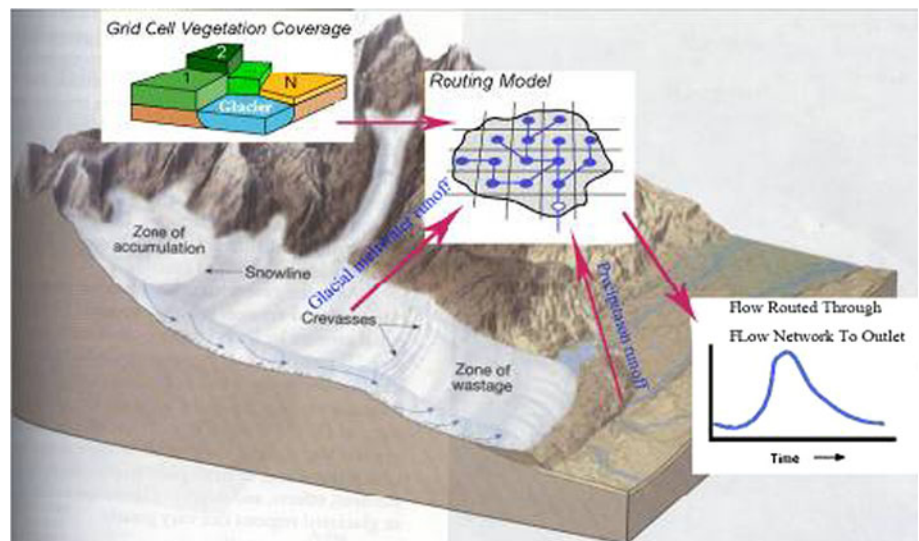
A glacier scheme was developed within the framework of the VIC macroscale hydrology model. The glacier algorithm in the VIC model is described by adding one special land use/land cover class to the grid cell mosaic as well as the vegetation and bare soil land classes (Fig. 1). Energy and mass balance of the glacier are resolved at each model time step. The glacier algorithm is based on the works of Hock (2005) and Jiang (2008).

**The VIC macroscale hydrological model**

The VIC model is a semi-distributed, grid-based macroscale hydrologic model (Liang et al. 1994; Nijssen et al. 1997, 2001) that adopts the VIC curve to describe the distribution of soil moisture, and considers explicitly the effects of vegetation, topography, and soils on the exchange of moisture and energy between land and atmosphere. It has been applied at spatial scales from 1/8° or less to several degrees latitude by longitude, and the temporal resolution of the model ranges from hourly to daily. One distinguishing characteristic of the VIC model is its use of a “mosaic” scheme. Statistical representation of the sub-grid scale spatial variability in topography and vegetation/land cover was applied in the VIC model. The use of statistical representation is important when simulating the accumulation and ablation of snow in a complex terrain. Early simulations with the VIC model were conducted using two soil layers. Liang et al. (1996) determined that the specification of a thin top layer (5–15 cm) in the model significantly improved evapotranspiration predictions in arid climates. Therefore, a third soil layer was added, with the modified VIC model being called the VIC-3L model, while the soil column was divided into more than ten layers when the model simulated frozen soil.

Evapotranspiration was calculated using the Penman–Monteith equation (Shuttleworth 1993). The snowpack within the VIC model was modeled as two layers of variable thickness. Snowpack dynamics were simulated by an energy and mass-balance model (Cherkauer and Lettenmaier 2003). The surface layer was used to represent the energy balance between the atmosphere and the snowpack, while the lower layer was used to solve processes within deeper snowpacks, and the lower layer was assumed to serve as storage for the excess snow mass derived from the

**Fig. 1** Schematic representation of the VIC glacier scheme



thin surface layer (Wigmosta et al. 1994). Surface runoff was generated according to the variable infiltration curve. The main factors depend on the infiltration capacity, which represents the spatial distribution of surface soil moisture (Liang et al. 1994). Baseflow was generated according to an empirically based nonlinear soil moisture relationship (Liang et al. 1994). The effects of frozen soil on infiltration and runoff were represented using the method developed by Cherkauer and Lettenmaier (1999, 2003). Surface runoff and baseflow for each cell were routed to the basin outlet through a channel network as described by Lohmann et al. (1998a, b), and the fraction of each grid cell at the edge of the basin flowing into the basin was taken into account (Nijssen et al. 1997).

Primary input data included daily precipitation and maximum and minimum daily temperatures. These were modeled or partitioned to the model time step. If radiation data and vapor pressure data were unavailable, these data were calculated by the model based on daily precipitation and daily minimum and maximum temperatures, using the algorithms developed by Thornton and Running (1999). If wind speed was not provided, the default values ( $1.5 \text{ m s}^{-1}$ ) were assumed. The air pressure was calculated by the pressure lapse rate from sea-level pressure (Mesinger and Treadon 1995) or using default values (95.5 kPa) when air pressure was unavailable.

#### Model development: glacier scheme

##### *Sub-grid variability in meteorological elements*

Most glaciers are distributed in high-altitude complex terrains. The meteorological conditions (temperature, precipitation, wind speed, radiation and others) of a glacier area are largely different from the macroscale model grid-cell mean. Therefore, a sub-grid representation of meteorological elements must first be adopted based on topography. In this study, average terrain information (slope, aspect and elevation) of the glacier area within a model grid-cell was statistically derived from the Advanced Spaceborne Thermal Emission and Reflection Radiometer (ASTER) Global Digital Elevation Model (GDEM) (<http://www.gdem.aster.ersdac.or.jp/>), 30-m resolution digital elevation data that are available globally. Although there are some data deficiencies in the ASTER GDEM for mountain areas, it can be used to obtain the altitude of glacier areas. The atmosphere pressure in a glacier area can be calculated by the pressure lapse rate from sea-level pressure based on the glacier area mean elevation.

The temperature (maximum and minimum) of the glacier area can be computed by the gradient method:

$$T_g = T_0 + l \times (Z_g - Z_0) \quad (1)$$

where  $T_g$  is the glacier area temperature ( $^{\circ}\text{C}$ ),  $Z_g$  (m) is the glacier area mean elevation,  $Z_0$  (m) is the grid-cell mean elevation,  $l$  is the temperature gradient ( $^{\circ}\text{C m}^{-1}$ ) that can be derived from observation.  $T_0$  is the grid-cell mean (and median) temperature ( $^{\circ}\text{C}$ ), which is represented using the gradient plus the inverse distance weighting interpolation from station observations to the grid-cell centers.

If shortwave radiation and the daily dew point temperature were not provided, they were calculated using the MT-CLIM (Mountain Climate Simulator, Thornton and Running 1999). However, the effects of slope and aspect on solar radiation are neglected during calculating the large-scale grid-cell mean shortwave radiation in the original version of the VIC model. Considering the effects of complex terrain in glacier area to solar radiation, the glacier area mean slope and aspect were reintroduced when calculating the shortwave radiation of glacier area.

##### *Energy and mass-balance of the glacier area*

Glacier melt is determined by the energy balance at the glacier-atmosphere interface, which is controlled by the meteorological conditions above the glacier and the physical properties of the glacier itself. A physically based approach to compute melt involves the assessment of the energy fluxes to or from the surface. When glacier surface temperature equals  $0^{\circ}\text{C}$ , any surplus of energy at the glacier surface-air interface is assumed to be used immediately for melting. The main formula of the mass-balance model is as follows, Mass ( $\text{kg m}^{-2}$ ):

$$\text{Mass} = \int \left( \frac{Q_M}{L_M} + P + \frac{Q_L}{L_S} \right) dt \quad (2)$$

where  $Q_M$  ( $\text{W m}^{-2}$ ) is the melt energy involved in melting,  $P$  (m) is the snow accumulation and  $Q_L$  ( $\text{W m}^{-2}$ ) represents the mass exchange due to sublimation.  $L_M$  ( $3.34 \times 10^5 \text{ J kg}^{-1}$ ) is the latent heat of melting, and  $L_S$  ( $2.83 \times 10^6 \text{ J kg}^{-1}$ ) is the latent heat of sublimation.

$Q_M$  was calculated from the glacier surface-energy balance and can be expressed as:

$$Q_N + Q_H + Q_L + Q_R + Q_G + Q_M = 0 \quad (3)$$

where  $Q_N$  ( $\text{W m}^{-2}$ ) is net radiation,  $Q_H$  ( $\text{W m}^{-2}$ ) is the sensible heat flux,  $Q_L$  ( $\text{W m}^{-2}$ ) is the latent-heat flux ( $Q_H$  and  $Q_L$  are referred to as turbulent heat fluxes),  $Q_G$  ( $\text{W m}^{-2}$ ) is the ground heat flux in the ice or snow, i.e., the heat exchange in a vertical column from the surface to the depth at which vertical heat transfer is negligible,  $Q_R$  ( $\text{W m}^{-2}$ ) is the heat flux supplied by precipitation and  $Q_M$  ( $\text{W m}^{-2}$ ) is the energy consumed by melt. As commonly defined in glaciology, a positive sign indicates an energy gain to the surface while a negative sign signifies an energy loss.

Net radiation of a surface is the difference between the incoming and outgoing energy absorbed or emitted by the surface. The net radiation may be written as:

$$Q_N = S(1-\alpha) + L\downarrow - L\uparrow \tag{4}$$

where  $S$  ( $\text{W m}^{-2}$ ) is global shortwave radiation,  $\alpha$  is albedo,  $L\downarrow$  ( $\text{W m}^{-2}$ ) is incoming longwave radiation (atmosphere longwave radiation) and  $L\uparrow$  ( $\text{W m}^{-2}$ ) is the emitted longwave radiation.

The albedo  $\alpha$  depends on the characteristics of the glacier surface including wetness, grain size, snow age, snow depth, and snow density. In this study, the snow albedo calculation based on the albedo algorithm developed by Gray and Landine (1987) as described by Sun et al. (1999) was used. In contrast to snow albedo, ice albedo is often treated as a temporal and spatial constant. Some studies suggest that there is a good relationship between ice albedo and daily air temperature (Jiang 2008), and in our study, the ice albedo algorithm was adopted.

$$\alpha_g = 0.324 - 0.018T_a \tag{5}$$

where  $\alpha_g$  is the ice albedo and  $T_a$  ( $^{\circ}\text{C}$ ) is the temperature. Considering the gap of glacier surface albedo between a fixed or variable snow value and a lower fixed ice value as soon as snow has melted completely, a function was introduced based on Brock et al. (2000).

$$\alpha = \alpha_s(1 - \exp(-d/d^*)) + \alpha_g \exp(-d/d^*) \tag{6}$$

where  $\alpha$  is the glacier surface albedo,  $\alpha_s$  is the snow albedo,  $\alpha_g$  is the ice albedo and  $d$  (mm w.e.) is the snow water equivalent which is calculated from snow accumulation and melt over the ice surface solved using the VIC two-layer energy-balance snow model (Cherkauer and Lettenmaier 2003), and  $d^*$  is the scale length for  $d$  (24 mm w.e.).

The incoming longwave radiation  $L\downarrow$  is estimated based on the fractional cloud cover, the current air temperature, and the atmospheric vapor pressure within the VIC model (Bras1990):

$$L\downarrow = L\downarrow_c (1 + 0.17c^2) \tag{7}$$

$$L\downarrow_c = \epsilon_a \sigma (T_a + 273.15)^4 \tag{8}$$

$$\epsilon_a = (1 + 0.17c^2)(0.740 + 0.000049V_p) \tag{9}$$

where  $L\downarrow_c$  is the clear-sky downward longwave radiation,  $c$  is the fractional cloud cover,  $\epsilon_a$  is the so-called effective clear-sky atmospheric emissivity,  $\sigma$  is the Stefan–Boltzmann constant,  $T_a$  is the air temperature ( $^{\circ}\text{C}$ ) and  $V_p$  is the vapor pressure (Pa).

Outgoing longwave radiation  $L\uparrow$  is approximated by

$$L\uparrow = \epsilon \sigma (T_0 + 273.15)^4 \tag{10}$$

where  $\epsilon$  is the emissivity of the surface (assumed to be 1),  $\sigma$  is the Stefan–Boltzmann constant and  $T_0$  is the temperature ( $^{\circ}\text{C}$ ) of the glacier surface. The surface temperature is assumed to be zero if the energy available for melt is positive. If melt turns negative, the surface temperature is calculated using the Brent iteration method (Brent 1973), which has been embedded in the VIC model.

The turbulent heat fluxes ( $Q_H$  and  $Q_L$ ) are calculated from the bulk aerodynamic method, assuming the sensible and latent-heat flux to be proportional to air temperature, wind speed and vapor pressure at a designated height above the surface, as described by Hock (2005) and Hock and Holmgren (2005):

$$Q_H = \rho c_p \frac{k^2}{[\ln(z/z_0) - \Psi_M(z/L)][\ln(z/z_{0T}) - \Psi_H(z/L)]} \times u(T_z - T_0) \tag{11}$$

$$Q_L = L_v \frac{0.622}{P} \frac{k^2}{[\ln(z/z_0) - \Psi_M(z/L)][\ln(z/z_{0e}) - \Psi_E(z/L)]} \times u(e_z - e_0) \tag{12}$$

where  $\rho$  is the air density,  $u$  is wind speed (m/s),  $c_p$  is the specific heat capacity of air ( $\text{J kg}^{-1} \text{K}^{-1}$ ),  $P$  is the atmospheric pressure (Pa),  $k$  is von Kármán constant (0.4),  $T_0$  is the surface temperature (K),  $e_0$  is the vapour pressure of the surface (Pa),  $z_0$ ,  $z_{0T}$  and  $z_{0e}$  are the roughness lengths for logarithmic profiles of wind speed, temperature and water vapour, respectively,  $\Psi_M$ ,  $\Psi_H$  and  $\Psi_E$  are the stability functions,  $L$  is the Monin–Obukhov length, and  $L_v$  is the latent heat of evaporation ( $2.514 \times 10^6 \text{ J kg}^{-1}$ ) or sublimation ( $2.849 \times 10^6 \text{ J kg}^{-1}$ ) as appropriate. Under neutral conditions, the functions  $\Psi$  assume a value of zero. The roughness lengths for temperature  $z_{0T}$  and vapour pressure  $z_{0e}$  are scaling parameters lacking a well-defined physical meaning. The stability functions  $\Psi$  depend on the stability parameter  $z/L$ , which in the stable boundary layer can be interpreted as the height at which the rate of turbulent energy production by shear stress balances the energy consumption by buoyancy forces (Anderas 1987, 2002). The detailed design and calculations can be found in Hock (2005).

Precipitation occurring below a threshold temperature is assumed to be snow. The model accounts for the energy advected by rain  $Q_R$  calculated by

$$Q_R = \rho_w c_w R (T_R - T_s) \tag{13}$$

where  $\rho_w$  is the density of water ( $\text{kg m}^{-3}$ ),  $c_w$  is the specific heat of water ( $4.18 \text{ kJ kg}^{-1} \text{K}^{-1}$ ),  $R$  is the rainfall rate ( $\text{m s}^{-1}$ ) and  $T_R$  ( $^{\circ}\text{C}$ ) and  $T_s$  ( $^{\circ}\text{C}$ ) are the temperatures of precipitation (assumed to be equal to air temperature) and the surface, respectively.  $T_R$  becomes equal to  $T_s$  before rain leaves the glacier surface.

Some studies and observations showed that the ground heat flux was approximately 0–5 W m<sup>-2</sup> after the ice had been exposed (Hock and Holmgren 1996; Jiang 2008). The amount is small, but because the direction of the flux is constant, neglect of the flux would introduce a systematic error (Hock and Holmgren 2005). Therefore, in this study, the ground-heat flux is approximated by assuming that it drops from 5 to 0 W m<sup>-2</sup> between the 1 July and 1 September, with between values determined using linear interpolation.

### Model calibration

As described above, the VIC-3L model contains a number of optimizable parameters which are used to adjust the model to the conditions prevailing in a specific catchment. Although most of the vegetation and soil parameters can be estimated according to the literature, some soil parameters are subject to calibration based on the agreement between simulated and observed hydrographs. These include the infiltration parameter (*b\_infil*), which controls the amount of water that can infiltrate into the soil; the depths of the three soil layers *d<sub>i</sub>* (*i* = 1, 2, 3), which affect the maximum storage available for transpiration; the three parameters in the baseflow scheme including the maximum velocity of baseflow (*D<sub>smax</sub>*), the fraction of maximum baseflow (*D<sub>s</sub>*), and the fraction of maximum soil moisture content of the third layer (*W<sub>s</sub>*) at which a nonlinear baseflow response is initiated, which determines how quickly the water stored in the third layer is depleted.

The parameters most often adjusted during calibration of the VIC model include, *b\_infil*, *D<sub>s</sub>*, *W<sub>s</sub>*, *D<sub>smax</sub>* and the depth of the second soil layer (Xie and Yuan 2006; Huang and Liang 2006). In this study, calibration was made manually and the Nash–Sutcliffe model efficiency coefficient (*R*<sup>2</sup>) (Nash and Sutcliffe 1970) was used as the objective function, which describes the matching extent of the hydrograph between the simulated and observed values:

$$R^2 = 1 - \frac{\sum_{i=1}^n (Q_{obs} - Q_{mod})^2}{\sum_{i=1}^n (Q_{obs} - \bar{Q}_{obs})^2} \quad (14)$$

where *Q<sub>obs</sub>*, *Q<sub>mod</sub>* are observed and simulated daily discharges, respectively,  $\bar{Q}_{obs}$  is the mean observed discharge and *n* is the total number of time steps.

Model calibration was performed by using the following procedures:

1. The model parameters (*D<sub>s</sub>* and *D<sub>smax</sub>*) were calibrated to fit the baseflow that occurred from the lowest soil layer.
2. The infiltration parameter *b\_infil* was adjusted to match the observed flow peaks, with a higher value

chosen to give lower infiltration and yield higher surface runoff.

3. A higher value of *W<sub>s</sub>* was chosen to raise the water content required for rapidly increasing, non-linear baseflow, which would tend to delay runoff peaks.
4. The estimated value for the depth of the soil layers (*d<sub>2</sub>*, *d<sub>3</sub>*) was set, commonly with a deeper depth for arid regions and a lower depth for humid regions.

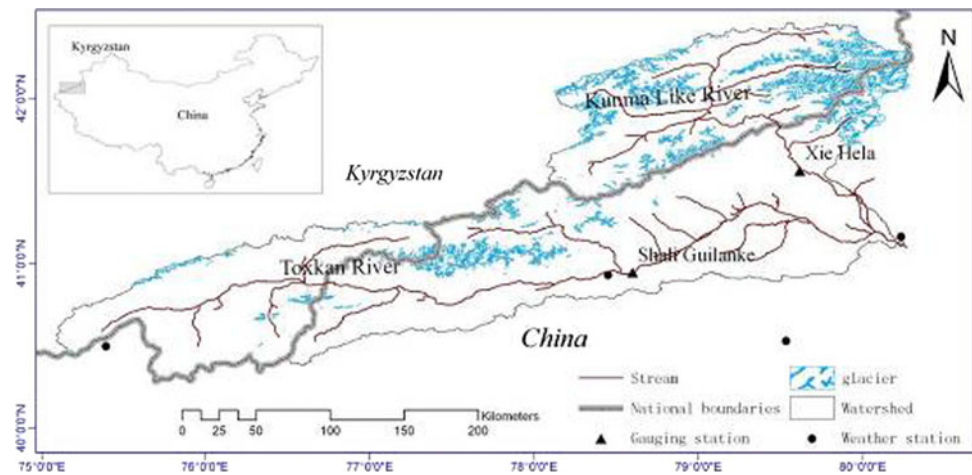
### Study area and data

#### Study area

The Aksu River basin (the international river between China and Kirghiz) lies to the north-west of the arid area of Tarim Basin, which is bounded by 75°08'E–80°13'E, 40°20'N–42°25'N (Fig. 2). The catchment area is 4.2 × 10<sup>4</sup> km<sup>2</sup> (3.7 × 10<sup>3</sup> km<sup>2</sup> glaciated). It is the most important headstream of Tarim Basin, contributing 73 % of the total streamflow of the main stream of the Tarim River. Vast territory, diverse topography, complex terrain and evident regional climate variations make up the characteristics of the north-west mountain climate. The high-mountain zone has lower temperatures, plentiful precipitation and aged snow while the middle-mountain zone brings about clear changes in temperature and is the largest precipitation distribution area. The low-mountain zone suffers from drought, large temperature fluctuations, and is fairly well represented in heat conditions, which reflects typical characteristics of dry continental climate such as minimal precipitation, intense evaporation, adequate sunshine, and extreme heat (Tang et al. 1992).

The Kunma Like and Toxkan Rivers converge to form the Aksu River. The Kunma Like River district, where the Termier and Hantengere Mountain glaciers come together, spans 293 km from the source to the point where the river converges. The hydrological station Xie Hela, controls a catchment area of 1.33 × 10<sup>4</sup> km<sup>2</sup> (2.8 × 10<sup>3</sup> km<sup>2</sup> glaciated). The Toxkan River spans 457 km from the source to the area where the Kunma Like River converges. In its mountain pass, the Shali Guilanke hydrological station covers a catchment area larger than 1.94 × 10<sup>4</sup> km<sup>2</sup> (9.0 × 10<sup>2</sup> km<sup>2</sup> glaciated). The Aksu River represents the rivers for which the glacial and snowmelt water are the primary source of water supply. The combination of ice/snow-melt and precipitation in summer forms the hydrological discharge process in the flood seasons of the Aksu River basin. Some studies have shown that the hydrological discharge process is so sensitive to climate change that it is necessary to study the relationship between the river's streamflow and climate (Shi et al. 2002; Jiang et al. 2005).

**Fig. 2** Location of the Aksu River basin, the stations and glaciers



**Data description**

The time-series daily atmospheric forcing data (maximum and minimum temperature, precipitation, and wind speed) for the period of 1970–2007, topography and land cover classification (elevation, vegetation, soil) and parameters were required for running the VIC hydrological model.

The daily temperature data of the study area were obtained from neighboring meteorological stations of the Chinese Meteorological Institute and interpolated to each model grid cell (at 5 min × 5 min spatial resolution) using a gradient plus inverse distance weighting method:

$$T_j = \frac{\sum_{i=1}^n (T_i \cdot d_i^{-2})}{\sum_{i=1}^n d_{ij}^{-2} + \left[ Z_j - \sum_{i=1}^n (Z_i d_{ij}^{-2}) / \sum_{i=1}^n d_{ij}^{-2} \right] G} \tag{15}$$

where  $T_j$  is the predicted temperature at grid point  $j$ ;  $T_i$  is the observed temperature of a neighboring weather station  $i$ ;  $d_{ij}$  is the distance between weather station  $i$  and grid point  $j$ ; and  $Z_j$  is the elevation of grid point  $j$ ;  $Z_i$  is the elevation of weather station  $i$ ;  $G$  is lapse rate of temperature which is obtained by observed data.

The precipitation data were obtained from a daily gridded precipitation dataset (APHRO\_V0902 datasets on  $0.25^\circ \times 0.25^\circ$  grids) which was created by the project of the Asian Precipitation Highly Resolved Observational Data Integration Towards the Evaluation of Water Resources (APHRODITE) (Yatagai et al. 2009). The precipitation data were interpolated to 5-min spatial resolution using the inverse distance weighing method.

Soil property data such as soil type, water-holding capacity and saturated hydrologic conductivity were sourced from the Food and Agriculture Organization (FAO) Soil Database, which provides the most detailed, globally consistent soil data (FAO-Unesco 1971–1981; Webb et al. 1993). The vegetation classification and their

parameters (including monthly leaf area index and albedo) were obtained from the University of Maryland’s 1 km Global Land Cover product. The proportion of each vegetation type in a covered grid cell was defined statically with GIS. Basic topography data were sourced from the global 30" GLOBE-DTM. The 30" Shuttle Radar Topography Mission DTM (Farr et al. 2007) was used to create the routing model input files, including the gridded fraction file concerning the fraction of each grid cell that flows into the basin being routed, and the gridded flow direction file which informs the routing model how all of the grid cells are connected in routing net.

The Chinese catchment glacier data were sourced from Chinese Glacier Inventory, which contains information about 26,000 glaciers throughout China, collected and digitized by the Cold and Arid Regions Environmental and Engineering Research Institute, CAS. The glacier data of the catchment in Kyrgyzstan were based on Landsat TM (1989–1993) remote sensing data. The topography of glaciers (elevation, slope and aspect) was obtained from 10" ASTER GDEM. The proportion of glacier in each covered grid cell and topographical information of glaciers, such as mean elevation, slope and aspect, were defined statically

Daily discharge data (1980–1989) and monthly discharge data (1970–2007) for the Aksu catchments were obtained from the Xinjiang Uygur Autonomous Region Hydrological Institute and used for the calibration and analysis of the VIC model.

**Results and discussion**

In this paper, the related typical parameters ( $b_{infiltr}$ ,  $D_s$ ,  $D_{smax}$ ,  $W_s$ ) were used as the starting values for the AKSU watersheds (<http://www.hydro.washington.edu/Lettenmaier/Models/VIC/Documentation/SoilParam.shtml>). The daily observed discharge data over the period 1980–1989 was

chosen for model calibration and parameter optimization. The VIC model has six main parameters to calibrate:  $D_{\text{max}}$ ,  $D_s$ ,  $W_s$  and  $d_3$  were adjusted based on the observed daily discharge in the cold season and  $b_{\text{infiltr}}$  and  $d_2$  were optimized based on the observed discharge on a rainy day. The VIC model has no automated optimization function, which makes the parameter optimization difficult. Eventually, the best daily simulation results were obtained by manual adjustment of parameters.

#### Discharge simulations

To further clarify the model performance of the VIC model, the modeled daily and monthly streamflows were compared with measurements from the stream gauge records for the calibration period 1980–1989 and the complete period 1970–2007 (Figs. 4, 5), and the statistical test is listed in Table 1. From the figures and table, the following conclusions can be made.

1. The previous VIC model without a glacier scheme systematically underestimated the streamflows, especially for the Kunma Like River catchment that has a higher glacier extent (Figs. 3, 4). The Nash–Sutcliffe model efficiency coefficients of  $R^2$  were small, only 0.46 for the Toxkan River and 0.34 for the Kunma Like River for the calibration period. The performances of the monthly runoff simulation for the complete period (1970–2007), using the previous VIC model, were in addition not satisfying, with a  $R^2$  of 0.42 for the Toxkan River and 0.35 for the Kunma Like River. Because glacial-melt water is the main component of the hydrological cycle in the Aksu catchment, glacier hydrology must be considered in hydrological modeling for a watershed with a high glacier extent, and the model performance cannot be improved just by parameter optimization of the model system.
2. The model performance was obviously improved through coupling a glacier-melt scheme. The improved

model achieved the efficiency coefficients of  $R^2 = 0.62$  for the Toxkan River and  $R^2 = 0.77$  for the Kunma Like River for the calibration period, and a  $R^2 = 0.77$  for the Toxkan River and  $R^2 = 0.87$  for the Kunma Like River for the complete period. The  $R^2$  for the Kunma Like River (higher glacier extent) was greater than that for the Toxkan River (lower glacier extent), which also indirectly further supports the glacier scheme. The simulated performances of monthly discharge were better than that of daily discharge.

3. The simulated discharge during the wet season had a slight tendency to underestimate the observations that can be seen from Fig. 3, and the model simulations undersimulate the highest observations. We inferred that the underestimations of the simulated discharges were mainly due to the lack of accurate spatial precipitation. Owing to the complexity of the spatial pattern of precipitation, the problem of accurately estimating areal precipitation in alpine regions remains.
4. In general, application of the extended VIC model coupled with the glacier scheme to the glaciated catchment area showed an acceptable model performance, and achieved an efficiency coefficient  $R^2 > 0.6$  for the calibration period and  $R^2 \approx 0.8$  for the complete period. From the analysis in this section, we can draw the conclusion that our designed glacier scheme is acceptable, and model performance was obviously improved. The simulated discharge can be used for further analysis.

#### Runoff components

In this paper, the total runoff was broken up into three components: glacial runoff (the runoff produced from melting ice of the glacier area), snowmelt runoff (surface runoff produced from melting snow) and rainfall runoff (including direct rainfall surface runoff and subsurface

**Table 1** Nash–Sutcliffe model efficiency coefficient  $R^2$  for the linear correlation between the modeled and measured runoff of the Aksu watershed

	Toxkan River		Kunma Like River	
	$R^2$ of calibration period	$R^2$ of complete period	$R^2$ of calibration period	$R^2$ of complete period
Simulating using previous VIC model without a glacier scheme	0.46	0.42	0.34	0.35
Simulating using improved VIC model with a glacier scheme	0.62	0.77	0.77	0.87
Glacier extent (%)	4.6		21.0	

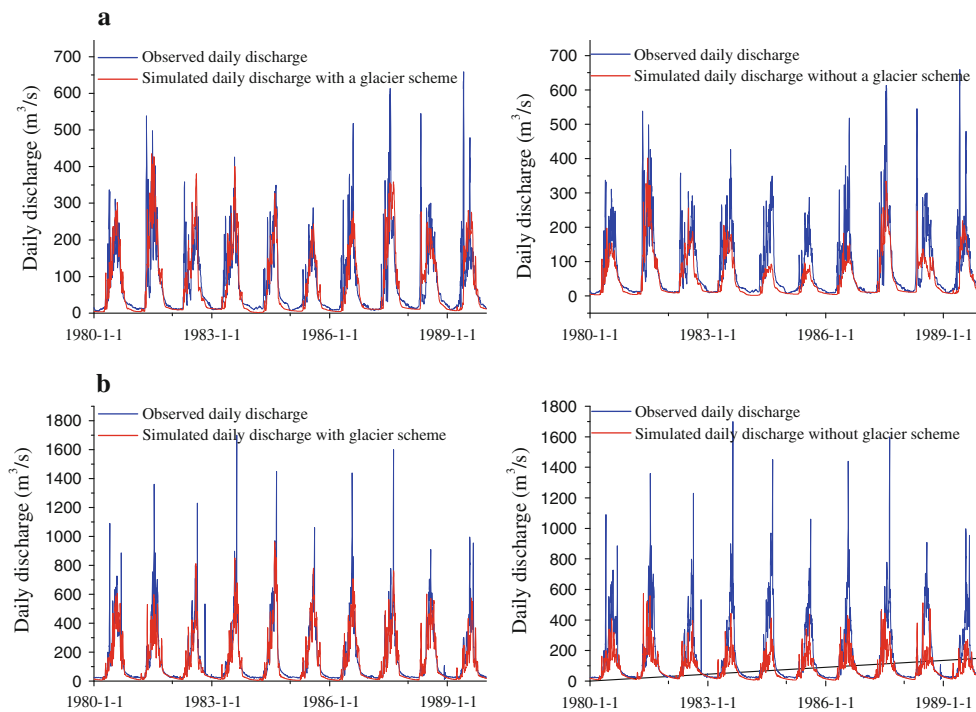


**Fig. 3** Observed and simulated daily discharge during the calibration period (1980–1989). **a** Toxkan river, **b** Kunma Like river

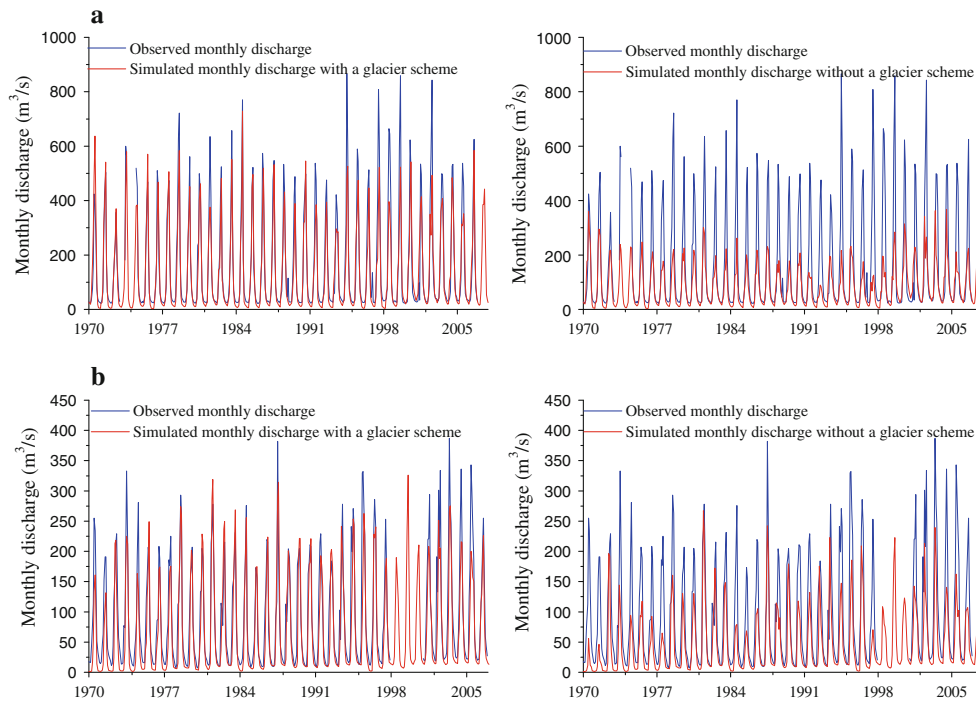


**Fig. 4** Observed and simulated monthly discharge (1970–2007). **a** Toxkan river, **b** Kunma Like river

runoff). Table 2 gives the sources of the two branches of the Aksu River, which indicates: the simulated average annual runoff of the two branches is in good agreement with the observations with a relative error of 6.1 % for the

Kunma Like River and 10.4 % for the Toxkan River; the average annual runoff of the Kunma Like River ( $48.67 \times 10^8 \text{ m}^3$ ) was greater than that of the Toxkan River ( $27.67 \times 10^8 \text{ m}^3$ ); ice meltwater accounted for a

**Table 2** Sources of Aksu River runoff

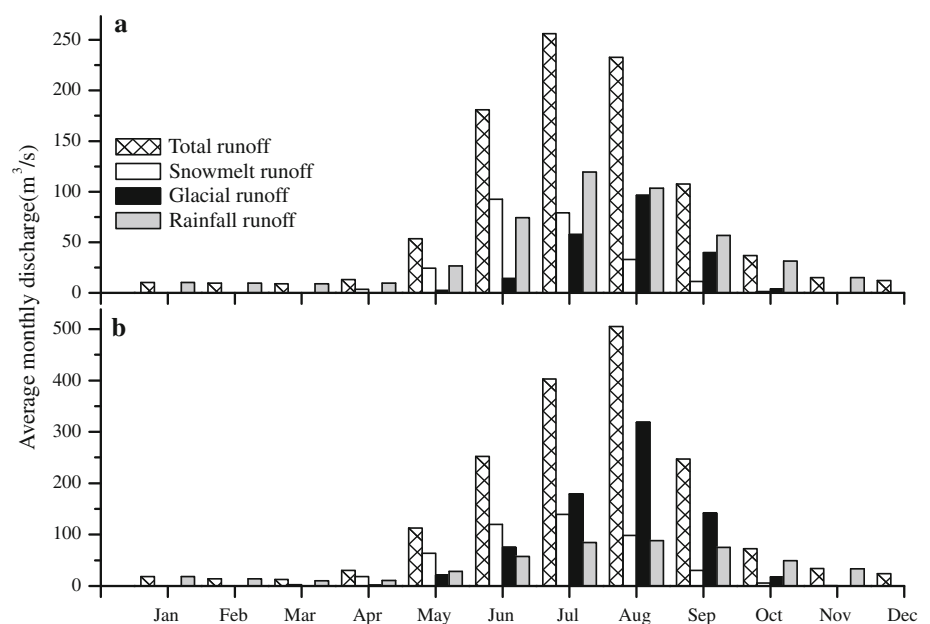
Branch name	Total runoff ( $10^8 \text{ m}^3$ )		From ice melt (%)	From snowmelt (%)	From rainfall and groundwater (%)
	Observation	Simulation			
Toxkan River	27.67	24.79	23.0	26.1	50.9
Kunma Like River	48.67	45.70	43.8	27.7	28.5

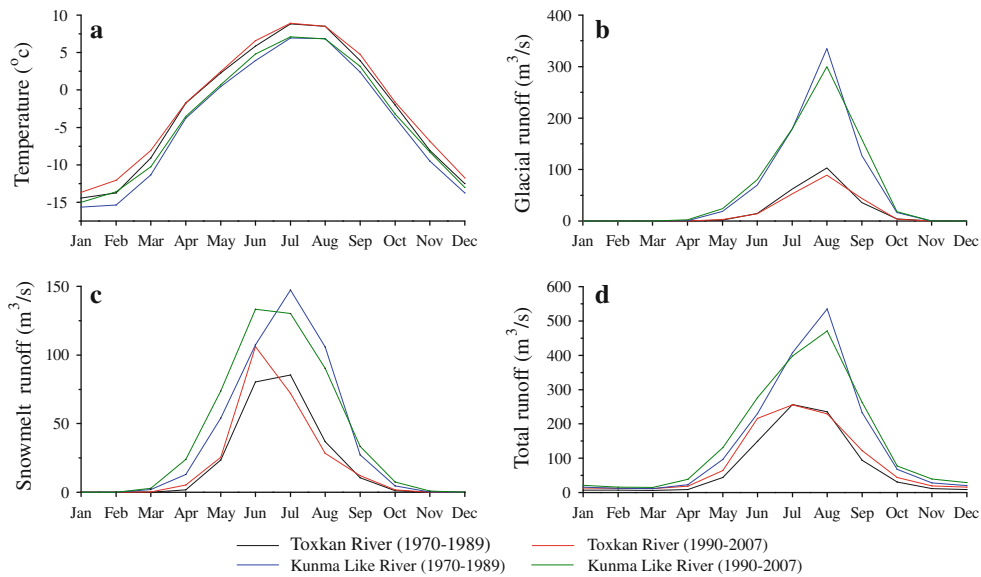
larger proportion of the Kunma Like River runoff (43.8 %) than that of the Toxkan River runoff (23.0 %); snowmelt water contributed 27.1 % of the Kunma Like River runoff and 26.7 % of the Toxkan River runoff; and the rainfall runoff of the Kunma Like River accounted for a smaller proportion (28.5 %) than that of Toxkan River (50.9 %). Previous studies (Chen et al. 2007; Shen et al. 2009) showed that meltwater (including snow and ice meltwater) of the glacier area recharges 24.7 % of the Toxkan River annual runoff, and 52.4 % of the Kunma Like River annual runoff. Hu (2004) pointed out that 74 % of the Kunma Like River annual runoff is from snow- and ice meltwater. Consistent with the previous results, our study showed that meltwater of the glacier area contributed 26.1 % of the Toxkan River annual runoff and 51.1 % of Kunma Like River annual runoff, snow and ice meltwater contributed 71.5 % of the Kunma Like River annual runoff.

Figure 5 presents the average monthly rates of runoff generation from the mode simulation. More than 88 % of the runoff volume occurred in the summer melt season (May to September), whereas runoff was negligible during winter when most precipitation was stored as snow. The ratio of maximum to mean monthly runoff of the Kunma Like River (3.5) was greater than that of the Toxkan River

(3.3), showing that the seasonal runoff intensity of the Kunma Like River was slightly higher than that of the Toxkan River. Comparing the plot of average monthly discharge, snowmelt ice melt, and rainfall of the Toxkan River and the Kunma Like River (see Fig. 5a, b), the main difference appears in July and August, when the peak time of total runoff shows differences. For the Toxkan River, the peak discharge occurs in July, while for the Kunma Like River, the peak discharge occurs in August. Detailed analysis showed that the ice melt is the driving factor for variation in the total runoff of the Kunma Like River, but precipitation is driving factor for variation in total runoff of the Toxkan River. In July and August, which is the main rainy and ice melt season, ice meltwater contributes about 44 and 63 % of the Kunma Like total runoff, while 92 and 78 % of the Toxkan River total runoff is derived from snowmelt and rainfall runoff. So that the peak time of the Kunma Like River total runoff is in keeping with that of glacial runoff (August), while the peak time of the Toxkan River total runoff is in accordance with that of precipitation runoff (July). The snowmelt water, which contributes about 43 % of total runoff in the Toxkan River and 55 % of the total runoff of the Kunma Like River during April–June, is an important source water resource.

**Fig. 5** Average monthly rates of runoff generation. **a** Toxkan River, **b** Kunma Like River





**Fig. 6** Change of runoff and air temperature of Aksu River from 1970 to 1990

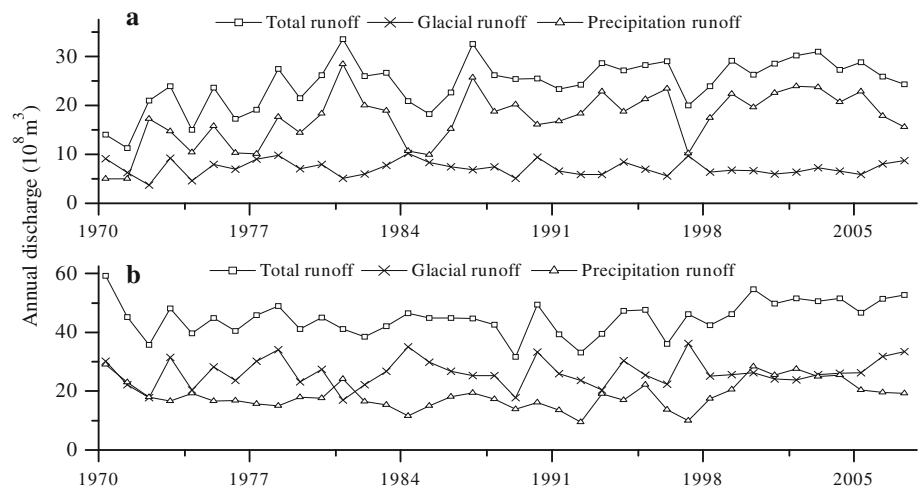
The varying characteristics of runoff

Figure 6 shows the variation in runoff and air temperature of the two branches from the 1970s (1970–1989) to the 1990s (1990–2007). As seen in Fig. 6a, the air temperature of two branches show an increasing trend in the years 1970–1990, rising about 0.8 °C in cold season (January–April and September–December) and 0.3 °C in warm season (May–August). Although the warm season average temperature has an increasing trend, the temperature in August shows a slight decreased trend (decreased by 0.01 °C). The impacts of climate warming on hydrology and water resources are shown on Fig. 6b–d. The rising temperature causes an earlier start and later end of the snow/ice melting period, resulting in a longer melting process. The change evident in glacial runoff is consistent with that of air temperature, with glacial runoff increasing during the melting season except for August, when the air temperature has a slight decreasing trend (Fig. 6b). The snowmelt runoff of the two branches increased obviously in spring and autumn and the peak time of snowmelt runoff has been advanced by a month during the 1970–1990, while snowmelt runoff in July and August showed an obvious decrease (Fig. 6c). Owing to the change of glacial and snowmelt runoff, the whole runoff process underwent a corresponding change. From the 1970–1990, the ratio of maximum to mean monthly total runoff of the Kunma Like River reduced from 3.8 to 3.2 and that of the Toxkan River also reduced from 3.6 to 3.0 (Fig. 6d).

Figure 7 shows the annual runoff process of the Aksu River. The annual total runoff variations of the two branches of the Aksu River were not identical. Due to the differences in glacier extent, the fluctuation of Toxkan River annual

total runoff was consistent with that of the non-glacial runoff, while the variation of the Kunma Like River annual total runoff was in agreement with that of glacial runoff. As evident in Fig. 7, it is obvious that the fluctuation of annual glacial runoff was opposite to that of the annual non-glacial runoff. In other words, the annual glacial runoff was smaller in wet years, while it was greater in dry years. That is because, the solar radiation is affected by precipitation frequency and vapor was lower in wet years, and a large amount of precipitation forms a thick snow pack on ice that results in slow snow/ice melt due to higher snow albedo. The phenomenon is generally referred to as the glacier compensation effect (Lang 1986): glaciers tend to dampen annual discharge variations, where ablation variations offset precipitation variations. In general, during the last 38 years, the fluctuations of annual total runoff of the two rivers had a positive trend. The Toxkan River average annual total runoff for period 2000–2007 was  $28.24 \times 10^8 \text{ m}^3$ , which was 44.9 % higher than that for the period 1970–1979 ( $19.49 \times 10^8 \text{ m}^3$ ) and increased by  $26.78 \times 10^6 \text{ m}^3$  per year. The Kunma Like River mean annual total runoff for period 2000–2007 was  $52.14 \times 10^8 \text{ m}^3$ , which was 13.6 % higher than that for period 1970–1979 ( $48.89 \times 10^8 \text{ m}^3$ ) and increased by  $12.86 \times 10^6 \text{ m}^3$  per year. Detailed analysis shows that the increase of precipitation runoff is the key driving factor for the increase of annual total runoff. For the Toxkan River, the annual runoff increased simply due to the increase in precipitation runoff (increased by  $28.7 \times 10^6 \text{ m}^3$  per year). For the Kunma Like River in the higher glacier extent catchment, 95.5 % of the increasing total runoff was from precipitation runoff (increased by  $12.28 \times 10^6 \text{ m}^3$  per year), and only 4.5 % from ice melt runoff (increased by  $0.58 \times 10^6 \text{ m}^3$  per year).

**Fig. 7** Varying characteristics of annual discharge (1970–2007). **a** Toxkan river, **b** Kunma Like river



## Conclusions

Although the characteristics and importance of glaciers and frozen soil in the land-surface hydrology of cold regions have long been recognized, surprisingly few hydrological models explicitly consider these processes. In this study, an energy-balance ice melt model was coupled to the VIC macroscale hydrological model (with a frozen soil and permafrost algorithm), considering the sub-grid variability in meteorological elements of glacier areas, to improve modeling performance in cold mountain catchments. The extended VIC model was applied to the glaciated catchment, Aksu River basin. The daily discharge data (1980–1989) of two hydrological stations (Shali Guilanke and Xie Hela) was used to calibrate the VIC model so as to optimize model parameters. Using these optimized parameters, the simulation achieved a Nash–Sutcliffe model efficiency coefficient of  $R^2 = 0.62$  for the Toxkan River and  $R^2 = 0.77$  for the Kunma Like River over the calibration period. The simulation of the monthly runoff for the complete period (1970–2007) also achieved desired results, with an efficiency coefficient of  $R^2 = 0.77$  obtained for the Toxkan River and  $R^2 = 0.87$  for the Kunma Like River. The simulated results show obvious improvement in the model performance through the coupling of the glacier scheme. The improved results demonstrate that it is necessary to consider glacier hydrology when modeling the mountain hydrological processes in the north-west China, especially in highly glaciated catchments. The numerical simulation test clearly demonstrated that the improved VIC model could accurately simulate the hydrological processes in a cold glaciated catchment. The glacier coupling methodology is a practical approach, and provides important references for the design of a glacier scheme in a macro-scale land surface model.

The analysis of the rates of runoff components (glacial runoff, snowmelt and rainfall runoff) shows that melting of the snow and ice is the major contribution to runoff (about 49.1 % for the Toxkan River and 71.5 % for the Kunma Like River) and that the seasonality of runoff of the Kunma Like River basin (3.5) is higher than that of the Toxkan River basin (3.3) due to different glacier extents. The varying characteristics of runoff are discussed. Warming of the climate increases the snow/ice melting rates and prolongs the melting period. The glacial and snowmelt runoff of the two branches increased obviously in spring and autumn, and the peak time of snowmelt runoff advanced by a month during the 1970–1990. Due to massive snow loss from the earlier melting period, the snowmelt runoff of July and August showed an obvious decrease. Owing to the changes to glacial runoff and snowmelt runoff, the seasonal runoff concentration reduces and the ratio of the maximum monthly total runoff to mean monthly total runoff decreases. The annual total runoff of the two branch of the Aksu River shows an increasing trend, increasing by 44.9 % for the Toxkan River and by 13.6 % for the Kunma Like River over the last 38 years. The increased precipitation runoff was the major factor causing the increase in the annual total runoff. The increase in the Toxkan River annual total runoff was simply due to the increased precipitation runoff, while 94.5 % of the increased Kunma Like River annual total runoff was from precipitation runoff, and only 5.5 % was from ice melt runoff. In conclusion, the research methodology contributes to the qualitative evaluation and forecast of water resource change, and provides reference for formulating the scientific sustainable development of water resources in north-western China.

It is noteworthy that the spatial distribution of precipitation is the key factor in hydrological modeling. Because of the complexity of the spatial pattern of precipitation and

mountain terrain, accurately estimating areal precipitation in Alpine regions still remains a scientific problem. The development of remote sensing and radar technology will benefit the sourcing of accurate areal precipitation for the simulation of mountain hydrological processes in the future.

**Acknowledgments** The work was supported by a grant from the Global Change Research Program of China (2010CB951404), the China National Natural Science Foundation (Grants Nos. 41030527, 41130641, 41130368 and 41001039) and the Foundation for Excellent Youth Scholars of CAREERI, CAS ( Grant No. 51Y251A61). We gratefully acknowledge the insightful comments of two anonymous reviewers.

## References

- Andreas EL (1987) A theory for the scalar roughness and the scalar transfer coefficients over snow and sea ice. *Bound Layer Meteorol* 38:159–184
- Andreas EL (2002) Parameterizing scalar transfer over snow and ice: a review. *J Hydrometeorol* 3:417–432
- Barnett TP, Adam JC, Lettenmaier DP (2005) Potential impacts of a warming climate on water availability in snow-dominated regions. *Nature* 438(7066):303–309
- Bayard D, Stähli M (2005) Effects of frozen soil on the groundwater recharge in Alpine areas. In: Jong C, Collins D, Ranzi R (eds) *Climate and hydrology in mountain areas*. Wiley, Chichester, pp 73–83
- Bergström S (1976) Development and application of a conceptual runoff model for Scandinavian catchments. Department of Water Resources Engineering, Lund Institute of Technology/University of Lund, Bulletin Series A 52, Swedish Meteorological and Hydrological Institute. Norrköping, Sweden
- Betts AK, Ball JH, Beljaars ACM, Miller MJ, Viterbo PA (1996) The land surface–atmosphere interaction: a review based on observational and global modeling perspectives. *J Geophys Res*. doi: [10.1029/95JD02135](https://doi.org/10.1029/95JD02135)
- Beven KJ (2001) *Rainfall runoff modeling*. Wiley, Chichester
- Bøggild CE, Knudby CJ, Knudsen MB, Starzer W (1999) Snowmelt and runoff modelling of an arctic hydrological basin in east Greenland. *Hydrol Proc* 13:1989–2002
- Bowling LC, Pomeroy JW, Lettenmaier DP (2004) Parameterization of blowing-snow sublimation in a macroscale hydrology model. *J Hydrometeorol* 5(5):745–762
- Bras RL (1990) *Hydrology: an introduction to hydrologic science*. Addison Wesley, New Jersey
- Braun LN, Weber M, Schulz M (2000) Consequences of climate change for runoff from Alpine regions. *Ann Glaciol* 31(1):19–25
- Brent RP (1973) *Algorithms for minimization without derivatives*. Prentice-Hall, Englewood Cliffs
- Brock BW, Willis IC, Sharp MJ (2000) Measurement and parameterization of albedo variations at Haut Glacier d’Arolla, Switzerland. *J Glaciol* 46(155):675–688
- Chen RS, Kang ES, Ji XB, Yang JP, Yang Y (2006) Cold regions in China. *Cold Reg Sci Technol* 45(2):95–102
- Chen Y, Hao X, Xu C (2007) The trend analysis of runoff change of Tarim River Basin, Xin Jang. *Sci Found China* 17(2):205–210 (In Chinese)
- Chen RS, Lü SH, Kang ES et al (2008) A distributed water-heat coupled model for mountainous watershed of an inland river basin of Northwest China (I) model structure and equations. *Environ Geol* 53(6):1299–1309
- Cherkauer KA, Lettenmaier DP (1999) Hydrologic effects of frozen soils in the upper Mississippi River basin. *J Geophys Res*. doi: [10.1029/1999JD900337](https://doi.org/10.1029/1999JD900337)
- Cherkauer KA, Lettenmaier DP (2003) Simulation of spatial variability in snow and frozen soil. *J Geophys Res*. doi: [10.1029/2003JD003575](https://doi.org/10.1029/2003JD003575)
- Christensen NS, Lettenmaier DP (2007) A multimodel ensemble approach to assessment of climate change impacts on the hydrology and water resources of the Colorado River Basin. *Hydrol Earth Syst Sci* 11(4):1417–1434
- Costa-Cabral MC, Richey JE, Goteti G et al (2008) Landscape structure and use, climate, and water movement in the Mekong River basin. *Hydrol Process* 22(12):1731–1746
- FAO-Unesco (1971–1981) *Soil map of the world: scale 1:5,000,000, vol 1 to vol 10*. United Nations Educational, Scientific, and Cultural Organization, Paris
- Farr TG, Rosen PA, Caro E, et al (2007) The Shuttle radar topography mission. *Rev Geophys*. doi: [10.1029/2005RG000183](https://doi.org/10.1029/2005RG000183)
- Flerchinger GN, Saxton KE (1989) Simulation heat and water model of a freezing snow-residue-soil system I. theory and development. *Trans ASAE* 32(2):565–571
- Gray DM, Landine PG (1987) Albedo model for shallow prairie snow covers. *Can J Earth Sci* 24(9):1760–1768
- Harlan RL (1973) Analysis of coupled heat-fluid transport in partially frozen soil. *Water Resour Res* 9(5):1314–1323
- Hastenrath S (1994) Recession of tropical glaciers. *Science* 265(5180):1790–1791
- Higuchi K (1976) *Glaciers and climates of Nepal Himalayas: report of the glaciological expedition to Nepal-Pt.1*. Japanese Society of Snow and Ice, Tokyo
- Higuchi K (1977) *Glaciers and climates of Nepal Himalayas: report of the glaciological expedition of Nepal-Pt. 2*. Japanese Society of Snow and Ice, Tokyo
- Higuchi K (1978) *Glaciers and climates of Nepal Himalayas: report of the glaciological expedition of Nepal-Pt. 3*. Japanese Society of Snow and Ice, Tokyo
- Higuchi K (1980) *Glaciers and climates of Nepal Himalayas: report of the glaciological expedition of Nepal-Pt. 4*. Japanese Society of Snow and Ice, Tokyo
- Hock R (1998) *Modelling of glacier melt and discharge: dissertation*. ETH, Zürich
- Hock R (2005) Glacier melt: a review of processes and their modeling. *Prog Phys Geogr* 29(3):362–391
- Hock R, Holmgren B (1996) Some aspects of energy balance and ablation of Storglaciären, northern Sweden. *Geogr Ann* 78A(2–3):121–131
- Hock R, Holmgren B (2005) A distributed surface energy-balance model for complex topography and its application to Storglaciären, Sweden. *J Glaciol* 51(172):25–36
- Hock R, Jansson P, Braun L (2005) Modeling the response of mountain glacier discharge to climate warming. In: Reasoner MA (ed) *Global change and mountain regions*. Springer, Netherlands, pp 243–252
- Hu YJ (2004) *Physical geography of the Tianshan Mountains in China*. China Environmental Science Press, Beijing (In Chinese)
- Huang M, Liang X (2006) On the assessment of the impact of reducing parameters and identification of parameter uncertainties for a hydrologic model with applications to ungauged basins. *J Hydrol* 320(1–2):37–61
- Jiang X (2008) *Model study of the surface energy and mass balance of Junly 1st Glacier at Qilian Mountains in China during the summer ablation period: dissertation*. Chinese Academy of Sciences, Beijing (In Chinese)
- Jiang Y, Zhou CH, Cheng WM (2005) Analysis on runoff supply and variation characteristics of Aksu drainage basin. *J Nat Resour* 20(1):27–34 (In Chinese)

- Kang ES, Cheng GD, Lan YC, Jin HJ (1999) A model for simulating the response of runoff from the mountainous watershed of inland river basins in the arid area of Northwest China to climatic changes. *Sci. China Ser D* 42(Suppl):52–63
- Kaser G, Juen I, Georges C et al (2003) The impact of glaciers on the runoff and the reconstruction of mass balance history from hydrological data in the tropical Cordillera. *J Hydrol* 282: 130–144
- Kayastha RB, Ageta Y, Nakawo M, Fujita K, Sakai A, Matsuda Y (2003) Positive degree-day factors for ice ablation on four glaciers in the Nepalese Himalaya and Qinghai-Tibetan Plateau. *Bull Glaciol Res* 20:7–14
- Lang H (1986) Forecasting meltwater runoff from snow-covered areas and from glacier basins. In: Kraijenhoff DA, Moll JR (eds) *River flow modelling and forecasting*. D Reidel Publishing, Dordrecht, pp 99–127
- Li X, Koike T (2003) Frozen soil parameterization in SiB2 and its validation with GAME-Tibet observations. *Cold Reg Sci Technol* 36(1–3):165–182
- Li X, Williams MW (2008) Snowmelt runoff modelling in an arid mountain watershed, Tarim Basin, China. *Hydrol Process* 22(19):3931–3940
- Liang X, Lettenmaier DP, Wood EF, Burges SJ (1994) A simple hydrologically based model of land surface water and energy fluxes for general circulation models. *J Geophys Res.* doi: [10.1029/94JD00483](https://doi.org/10.1029/94JD00483)
- Liang X, Wood EF, Lettenmaier DP (1996) Surface soil moisture parameterization of the VIC-2L model: evaluation and modification. *Glob Planet Change* 13(1–4):195–206
- Lohmann D, Raschke E, Nijssen B, Lettenmaier DP (1998a) Regional scale hydrology. I Formulation of the VIC-2L model coupled to a routing model. *Hydrol Sci J* 43(1):131–141
- Lohmann D, Raschke E, Nijssen B, Lettenmaier DP (1998b) Regional scale hydrology. II Application of the VIC-2L model to the Weser River, Germany. *Hydrol Sci J* 43(1):143–157
- Luo S, Lü S, Zhang Y (2009) Development and validation of the frozen soil parameterization scheme in Common Land Model. *Cold Reg Sci Technol* 55(1):130–140
- Martinez J, Rango A (1986) Parameter values for snowmelt runoff modeling. *J Hydrol* 84(3–4):197–219
- Mesinger F, Treadon RE (1995) “Horizontal” reduction of pressure to sea level: comparison against the NMC’s Shuell method. *Mon Weather Rev* 123(1):59–68
- Mölg T, Hardy DR (2004) Ablation and associated energy balance of a horizontal glacier surface on Kilimanjaro. *J Geophys Res.* doi: [10.1029/2003JD004338](https://doi.org/10.1029/2003JD004338)
- Nash JE, Sutcliffe JV (1970) River flow forecasting through conceptual models. Part I: a discussion of principles. *J Hydrol* 10(3):282–290
- Nicolisky DJ, Romanovsky VE, Alexeev VA, Lawrence DM (2007) Improved modeling of permafrost dynamics in a GCM land-surface scheme. *Geophys Res Lett.* doi: [10.1029/2007GL029525](https://doi.org/10.1029/2007GL029525)
- Nijssen B, Lettenmaier DP, Liang X, Wetzel SW, Wood EF (1997) Streamflow simulation for continental-scale river basins. *Water Resour Res* 33(4):711–724
- Nijssen B, Schnur R, Lettenmaier DP (2001) Global retrospective estimation of soil moisture using the Variable Infiltration Capacity landsurface model, 1980–1993. *J Clim* 14(8):1790–1808
- Quick MC, Pipes A (1977) UBC watershed model. *Hydrol Sci Bull* 22(1):153–161
- Rupper S, Roe G (2008) Glacier changes and regional climate: a mass and energy balance approach. *J Clim* 21(20):5384–5401
- Shen YP, Wang GY, Ding YJ et al (2009) Changes in glacier mass balance in watershed of Sary Jaz-Kumarik rivers of Tianshan Mountains in 1957–2006 and their impact on water resources and trend to end of the 21th century. *J Glaciol Geocryol* 31(5):92–800 (In Chinese)
- Shi YF, Shen YP, Hu RJ (2002) Preliminary study on signal, impact and foreground of climatic shift from warm–dry to warm–humid in Northwest China. *J Glaciol Geocryol* 24(3):219–226 (In Chinese)
- Shuttleworth WJ (1993) Evaporation. In: Maidment DR (ed) *Handbook of hydrology*, chap 4. McGraw Hill Inc, New York
- Singh P, Bengtsson L (2005) Impact of warmer climate on melt and evaporation for the rainfed, snowfed and glacierfed basins in the Himalayan region. *J Hydrol (Amst)* 300(1–4):140–154
- Smirnova TG, Brown JM, Benjamin SG, Kim D (2000) Parameterization of cold-season processes in the MAPS land-surface scheme. *J Geophys Res.* doi: [10.1029/1999JD901047](https://doi.org/10.1029/1999JD901047)
- Storck P (2000) *Trees, snow and flooding: an investigation of forest canopy effects on snow accumulation and melt at the plot and watershed scales in the Pacific Northwest*: dissertation. University of Washington, Washington, DC
- Sun S, Jin J, Xue Y (1999) A simple snow–atmosphere–soil transfer model. *J Geophys Res.* doi: [10.1029/1999JD900305](https://doi.org/10.1029/1999JD900305)
- Tang QC, Qu YG, Zhou YZ (1992) *Hydrology and water resources of arid area in china*. Science Press, Beijing (In Chinese)
- Tangborn WV (1984) Prediction of glacier derived runoff for hydroelectric development. *Geog Ann* 66A(3):257–265
- Thornton PE, Running SW (1999) An improved algorithm for estimating incident daily solar radiation from measurements of temperature, humidity, and precipitation. *Agric For Meteorol* 93(4):211–228
- Viviroli D, Dürr HH, Messerli B, Meybeck M, Weingartner R (2007) Mountains of the world, water towers for humanity: typology, mapping, and global significance. *Water Resour Res.* doi: [10.1029/2006WR005653](https://doi.org/10.1029/2006WR005653)
- Wang L, Koike T, Yang K, Jin R, Li H (2010) Frozen soil parameterization in a distributed biosphere hydrological model. *Hydrol Earth Syst Sci* 14(3):6895–6928
- Webb RS, Rosenzweig CE, Levine ER (1993) Specifying land surface characteristics in general circulation models: soil profile data set and derived water-holding capacities. *Global Biogeochem Cycles* 7(1):97–108
- Wigmosta MS, Vail LW, Lettenmaier DP (1994) A distributed hydrology-vegetation model for complex terrain. *Water Resour Res* 30(6):1665–1679
- WMO (1986) *Intercomparison of models of snowmelt runoff*. In: WMO (ed) *Operational Hydrology Report No 23*. WMO, Geneva (WMO-No 646)
- Xie Z, Yuan F (2006) A parameter estimation scheme of the land surface model VIC using the MOPEX databases. *IAHS Publication* 307:169–179
- Yang ZN, Liu XR, Zeng QZ, Chen ZT (2000) *Hydrology in cold regions of China*. Science Press, Beijing (In Chinese)
- Yatagai A, Arakawa O, Kamiguchi K et al (2009) A 44-Year daily gridded precipitation dataset for asia based on a dense network of rain gauges. *SOLA* 5:137–140
- Ye B, Yang D, Zhang Z, L. Kane D (2009) Variation of hydrological regime with permafrost coverage over Lena Basin in Siberia. *J Geophys Res.* doi: [10.1029/2008JD010537](https://doi.org/10.1029/2008JD010537)
- Yi S, Arain MA, Woo MK (2006) Modifications of a land surface scheme for improved simulation of ground freeze-thaw in northern environments. *Geophys Res Lett.* doi: [10.1029/2006GL026340](https://doi.org/10.1029/2006GL026340)
- Yi S, Woo Mk, Arain MA (2007) Impacts of peat and vegetation on permafrost degradation under climate warming. *Geophys Res Lett.* doi: [10.1029/2007GL030550](https://doi.org/10.1029/2007GL030550)
- Zhang Y, Liu SY, Ding YJ (2006) Observed degree-day factors and their spatial variation on glaciers in western China. *Ann Glaciol* 43(1):301–306

Zhang X, Sun S, Xue Y (2007) Development and testing of a frozen soil parameterization for cold region studies. *J Hydrometeorol* 8(4):690–701

Zhao Q, Liu Z, Ye B et al (2009) A snowmelt runoff forecasting model coupling WRF and DHSVM. *Hydrol Earth Syst Sci* 13(10):1897–1906